

"Made available under NASA sponsorship
in the interest of early and wide dis-
semination of Earth Resources Survey
Program information and without liability
for any use made thereof."

E7.4-10489
CR-136890

A TECHNIQUE FOR CORRECTING ERTS DATA
FOR SOLAR AND ATMOSPHERIC EFFECTS

Robert H. Rogers, Keith Peacock, N. J. Shah
Bendix Aerospace Systems Division
3300 Plymouth Road
Ann Arbor, Michigan 48107

April 1974
Special Report

Prepared for
GODDARD SPACE FLIGHT CENTER
Greenbelt, Maryland 20771

(E74-10489) A TECHNIQUE FOR CORRECTING
ERTS DATA FOR SOLAR AND ATMOSPHERIC
EFFECTS Special Report (Bendix Corp.)
21 p HC \$4.25 CSCL 05B
20

N74-22013

Unclas
G3/13 00489

TECHNICAL REPORT STANDARD TITLE PAGE

1. Report No.	2. Government Accession No.	3. Recipient's Catalog No.	
4. Title and Subtitle A Technique for Correcting ERTS Data for Solar and Atmospheric Effects		5. Report Date April 1974	
		6. Performing Organization Code	
7. Author(s) R. H. Rogers, K. Peacock and N. Shah		8. Performing Organization Report No.	
9. Performing Organization Name and Address Bendix Aerospace Systems Division 3300 Plymouth Road Ann Arbor, Michigan 48107		10. Work Unit No.	
		11. Contract or Grant No. NAS5-21863 MMC655	
12. Sponsoring Agency Name and Address NASA Goddard Space Flight Center Greenbelt, Md. 20771		13. Type of Report and Period Covered Special Report	
		14. Sponsoring Agency Code	
15. Supplementary Notes			
16. Abstract Based on processing ERTS CCTs and ground truth measurements collected on Michigan test site for January through June 1973 the following significant results are reported: (1) atmospheric transmittance varies from: 70 to 85% in Band 4, 77 to 90% in Band 5, 80 to 94% in Band 6, and 84 to 97% in Band 7 for one air mass, (2) a simple technique was established to determine atmospheric scattering seen by ERTS from ground-based measurements of sky radiance. For March this scattering was found to be equivalent to that produced by a target having a reflectance of 11% in Band 4, 5% in Band 5, 3% in Band 6, and 1% in Band 7, (3) computers ability to classify targets under various atmospheric conditions was determined. Classification accuracy on some targets (i. e., bare soil, tended grass, etc.) hold up even under the most severe atmospheres encountered, while performance on other targets (trees, urban, range-land, etc.) degrades rapidly when atmospheric conditions change by smallest amount.			
17. Key Words (Selected by Author(s)) Atmospheric parameters, Computer processing, ERTS-1		18. Distribution Statement	
19. Security Classif. (of this report) Unclassified	20. Security Classif. (of this page) Unclassified	21. No. of Pages 20	22. Price* 4.25

A TECHNIQUE FOR CORRECTING ERTS DATA FOR SOLAR AND ATMOSPHERIC EFFECTS

Robert H. Rogers, Keith Peacock, and Navinchandra J. Shah
Bendix Aerospace Systems Division
Ann Arbor, Michigan

ABSTRACT

A technique is described by which ERTS investigators can obtain and utilize solar and atmospheric parameters to transform spacecraft radiance measurements to absolute target reflectance signatures. A radiant power measuring instrument (RPMI) and its use in determining atmospheric parameters needed for ground truth are discussed. The procedures used and results achieved in processing ERTS CCTs to correct for atmospheric parameters to obtain imagery are reviewed. Examples are given which demonstrate the nature and magnitude of atmospheric effects on computer classification programs.

INTRODUCTION

The need for target reflectance signatures evolves from the needs of individual Principal Investigators, NASA's requirements to correlate results of a large number of investigators, and the pre-conditions of wide-area extrapolations of ground truth data for automatic data processing techniques. Target reflectance data are needed by all man and machine systems to obtain the unambiguous interpretation of ERTS data. In response to the need for absolute target reflectance signatures, this Experiment MMC 655 is evaluating the capabilities of a wide range of techniques for determining and removing solar and atmospheric parameters and effects from ERTS data. Techniques being evaluated include (1) transferring known ground reflectance to spacecraft measurements, (2) using the ground-based Radiant Power Measuring Instrument (RPMI) to measure, directly, the needed solar and atmospheric parameters, (3) using spacecraft data alone (with little or no auxiliary inputs), and (4) using radiation transfer models employing inputs such as surface pressure, ground visibility, temperature, and relative humidity. This paper evaluates the RPMI technique.

ATMOSPHERIC PARAMETERS

The desired reflectance information is difficult to obtain directly from the ERTS sensor radiance measurements because these measurements are a function of unknown solar and atmospheric parameters caused by the intervening atmosphere, and these parameters vary significantly. The radiance, L , sensed by the spacecraft sensor from a given target, depends not only upon the reflectance, ρ , of the target, but also upon the target irradiance, H , and upon the spectral absorption and scattering of the atmosphere between the target and the spacecraft. This atmosphere attenuates the radiance reflected from the target to the spacecraft and adds to the foreground radiance by backscatter of sunlight from the atmosphere, L_A . The composite radiance, L , recorded within an ERTS band for a spacecraft looking vertically is, therefore, related to the desired target reflectance, ρ , and to the solar and atmospheric parameters; H , τ , and L_A ; by:

$$L = \frac{\rho}{\pi} H \tau + L_A \quad (1)$$

where τ is the beam transmittance for one air mass.

The target irradiance, H , has two components; one caused by the direct sun, denoted $H_{\text{SUN}} \cos Z$ (in which H_{SUN} is the irradiance on a surface normal to the sun's rays and Z is the solar zenith angle) and a component caused by the sky, denoted H_{SKY} . Expanding H of Equation 1 in terms of the direct sun and sky components and solving the equation for ρ results in

$$\rho = \frac{(L - L_A) \cdot \pi}{\tau (H_{\text{SUN}} \cos Z + H_{\text{SKY}})} \quad (2)$$

For a remote sensing system looking vertically downward, τ is the atmospheric transmission of one air mass. If m is the number of air masses referenced to the zenith air mass (for which $m = 1$), the atmospheric transmission through some other value of m is given by τ^m . The direct sun component of target irradiance, H_{SUN} , in Equation 2 can be subdivided as

$$H_{\text{SUN}} = H_o \tau^m, \quad (3)$$

in terms of the solar irradiance normal to the sun's rays outside the atmosphere, H_o . Combining Equations 2 and 3, the desired target reflectance, ρ , in terms of ERTS radiance, L , measurements is

$$\rho = \frac{(L - L_A) \cdot \pi}{\tau (H_0 \tau^m \cos Z + H_{SKY})}, \quad (4)$$

where L_A , τ , H_0 , m , $\cos Z$, and H_{SKY} are the solar and atmospheric parameters that must be known to accurately compute target reflectance.

Parameters Readily Determined

In the machine processing of ERTS computer compatible tapes (CCTs), the parameters L , H_0 , m , and Z of Equation 4 are easily and quickly determined. Target counts, c_i , recorded on ERTS CCTs are transformed to the target radiance, L of Equation 4 by

$$L_i = c_i K_i \text{ mw/cm}^2 \text{ - sr}, \quad (5)$$

where i indicates MSS band number and constants K_i are determined as described on Page 6-14 of the ERTS Data User Handbook ($K_4 = 0.0195$, $K_5 = 0.0157$, $K_6 = 0.0138$, $K_7 = 0.0730$). The sun zenith angle, Z , is computed from $Z = 90 - \theta_E$, in which the sun elevation angle, θ_E , is also extracted from the ERTS CCT. For sun zenith angles less than 60 degrees, the air mass, m of Equation 4, is given to an accuracy better than 0.25% by $m = \sec Z$. For larger sun angles, a more accurate value is given by Bemporad's formula

$$M = \sec Z - 0.001867 (\sec Z - 1) - 0.002875 (\sec Z - 1)^2 - 0.0008083 (\sec Z - 1)^3. \quad (6)$$

The solar irradiance, H_0 , outside the earth's atmosphere is well known and changes less than 6% over a 12-month period. H_0 can be determined from NASA-published data (Thekaekara, 1971) or derived from RPMI measurements. Values obtained from RPMI and Dr. Thekaekara's published data for a mean earth-sun distance of 1 astronomical unit (AU), are shown in Table 1.*

If desired, the values specified (for 1 AU) can be corrected for the precise earth-sun distance at the time of ERTS overflight by factors also given in Dr. Thekaekara's report.

The remaining solar and atmospheric parameters needed for Equation 4; L_A , τ , and H_{SKY} ; depend on the specific atmosphere within the scene and must be determined by the Principal Investigator at the time of ERTS overflight.

* Please refer to back of report for tables, figures, and references.

RADIANT POWER MEASURING INSTRUMENT (RPMI)

One technique for obtaining the remaining atmospheric parameters is to deploy the RPMI shown in Figure 1. This instrument was developed specifically to provide an ERTS investigator with the capability of obtaining the complete set of solar and atmospheric measurements.

The RPMI is a rugged, hand-carried, portable instrument, calibrated to measure both down-welling and reflected radiation within each ERTS MSS band. A foldover handle permits a quick change from wide-angle global or sky irradiance measurements to narrow angle (7.0° circular) radiance measurements from sky and ground targets.

The RPMI's wide dynamic range (1 to 10^6) is tailored to permit measurements to be made over the full range of atmospheric parameters encountered by ERTS. These extremes have been found to include direct beam solar irradiance up to 25 mw/cm^2 in Band 7, sky radiance as low as $0.077 \text{ mw/cm}^2 - \text{sr}$ in Band 6, and radiance reflected from water surfaces in Bands 6 and 7 as low as $0.02 \text{ mw/cm}^2 - \text{sr}$. The RPMI measurements are traceable to an NBS source to an accuracy of 5% absolute and 2% relative from band-to-band. The RPMI calibration is also checked, from time to time, against the NASA Goddard calibration source to ensure uniformity between RPMI and ERTS MSS measurements.

DETERMINATION OF ATMOSPHERIC PARAMETERS

The RPMI is deployed in concert with ERTS overflights to obtain direct measurements, within the four ERTS MSS bands, of (1) global irradiance, H , (2) sky irradiance H_{SKY} , (3) radiance from a narrow solid angle of sky, $L_{\text{MEAS}}(\phi)$, and (4) direct beam-solar irradiance $H_{\text{SUN}}(m)$. From these measurements, additional solar and atmospheric parameters, such as beam transmittance, τ ; path radiance, L_A ; and direct beam-solar irradiance above the atmosphere, H_0 , are determined. With these parameters, Equation 4 is applied to transform the ERTS radiance measurements, L , into absolute target reflectance units.

DIRECT BEAM SOLAR IRRADIANCE (H_{SUN})

Direct beam solar irradiance, H_{SUN} , is measured, as shown in Figure 1C, by pointing the instrument directly at the sun with the telescope in place and recording the irradiance at each wavelength.

GLOBAL AND SKY IRRADIANCE

Global irradiance, H , is measured directly in each band as shown in Figure 1B. Additional accuracy in H can be obtained using H_{SUN} (m) and sky irradiance, H_{SKY} , by shadowing the sun and reading global minus direct beam-solar irradiance, and then computing the total target irradiance, using

$$H = H_{\text{SUN}} \cos Z + H_{\text{SKY}} \quad (7)$$

The sun angle, Z , may be read from the sun dial on the side of the RPMI after leveling the instrument with its bubble level.

BEAM TRANSMITTANCE (τ)

Beam transmittance, τ , per unit air mass is determined directly from

$$\tau = \left(\frac{H_{\text{SUN}}}{H_o} \right) \frac{1}{m} \quad (8)$$

when the solar irradiance outside the atmosphere, H_o , is known, as in Table 1. The air mass is calculated from the solar zenith angle, using Equation 6.

If solar irradiance outside the atmosphere, H_o , is not known, τ per unit air mass can be determined by making at least two H_{SUN} measurements, denoted $H_{\text{SUN}}(m_1)$ and $H_{\text{SUN}}(m_2)$, at air masses m_1 and m_2 and computing

$$\tau = \left(\frac{H_{\text{SUN}}(m_1)}{H_{\text{SUN}}(m_2)} \right) \frac{1}{m_1 - m_2} \quad (9)$$

If a series of $H_{\text{SUN}}(m)$ measurements are made and then plotted on a log scale as a function of air mass, an atmospheric extinction curve similar to that shown in Figure 2 results. By performing a least squares curve fit to the H_{SUN} measurements, greater accuracy in the H_{SUN} values needed for Equation 9 may be derived.

The intercepts of the H_{SUN} lines of Figure 2 with the vertical axis (i. e., $m = 0$) yields H_o in each ERTS band. These values of H_o can be used in succeeding computations of τ by Equation 8 and as calibration constants to test and recalibrate the RPMI, if necessary, using the sun as a source, at any location in the world.

Beam transmittance, τ , derived from 10 sets of field measurements covering the period January through June of 1973 (Table 2) shows this parameter to range from 70 to 85% in Band 4, from 77 to 90% in Band 5, from 81 to 94% in Band 6, and from 84 to 97% in Band 7.

PATH RADIANCE

The only remaining atmospheric parameter needed to transform ERTS radiance into reflectance is the radiance, L_A , reaching the spacecraft from Rayleigh and aerosol scattering by the atmosphere. As path radiance cannot be measured directly, it must be derived from ground-based sky radiance measurements of the backscatter. The simplest technique is to use the RPMI to measure the sky radiance, $L_{MEAS}(\phi)$, scattered at angle ϕ , as shown in Figure 3, such that ϕ is identical to ϕ , the angle through which radiation is scattered to the spacecraft, and then to correct this measurement for the difference in air masses between the direction of observation and the direction of the spacecraft. This technique provides a straightforward measurement procedure when $Z > 45^\circ$. When L_{MEAS} is recorded at an angle equal to the scattering angle to the ERTS, the path radiance, L_A , seen by ERTS is

$$L_A = L_{MEAS} \left(\frac{1 - \tau}{m_o} \right), \quad (10)$$

in which m_o is the air mass in the direction of observation (in this case $m_o = \frac{1}{\cos \beta}$) and τ , as previously defined, is the atmospheric transmission per unit air mass. The validity of this formula has been demonstrated by Rogers and Peacock (April 1973) and discussed by Gordon, Harris, and Duntley (1973). Equation 10 is adequate when the atmospheric measurements are made concurrent with the ERTS overflight; (i. e., at a sun angle close to the one at the time of the ERTS flyover).

However, if $Z < 45^\circ$, it is easy to see that $\beta > 90^\circ$ and a simple determination of L_A is not possible. During the summer months, this is frequently the condition at the time of the ERTS overpass. It becomes necessary to make the sky radiance measurements at a time when $Z > 45^\circ$ and to correct for the greater attenuation of the incident sunlight.

A correction factor, T_{ERTS}/T_Z , must be multiplied by Equation 10 to derive the path radiance, L_A , viewed by the spacecraft if the time between the ERTS overpass of the test site and the time of the sky radiance observations is significantly different. An approach for determining this correction factor was reported by Rogers and Peacock (October 1973) and is shown in Figure 3.

Sunlight entering the atmosphere at an angle Z , as shown in Figure 3, is scattered at altitude h in the direction of the observer at point 0. The energy available for scattering depends on the atmospheric extinction coefficient, $\tau_{\infty h}$, measured from outside the atmosphere to altitude h . The attenuation is given by $\exp(-\tau_{\infty h} \cdot m)$. The energy scattered is a function of the scattering coefficient, α_h , at altitude h . Thus, the energy scattered in the direction of the observer from altitude h is proportional to

$$\exp(-\tau_{\infty h} \cdot m) \cdot \alpha_h. \quad (11)$$

The average attenuation, for all altitudes, before the energy is scattered to the observer is given by

$$T = \frac{\sum_N \exp(-\tau_{\infty h} \cdot m) \cdot \alpha_h}{N \sum_N \alpha_h}, \quad (12)$$

in which N defines each atmospheric altitude used in the summation. Use of the value α_h in the equation expresses the importance of each altitude, h , in contributing energy at the observer location point, 0. A normalizing factor is included in the denominator. Values of $\tau_{\infty h}$ and α_h have been tabulated (Valley, 1965). To adjust $\tau_{\infty h}$ from a standard atmosphere to the actual atmospheric conditions at the observer's location, $\tau_{\infty h}$ is multiplied by $\exp(-\tau_{\infty 0})/\tau$, in which τ is the measured atmospheric transmission and $\tau_{\infty 0}$ is the extinction coefficient for a beam traversing one atmospheric air mass of a standard atmosphere. This is also given by Valley (1965). Variations in T are small, so the error in using a corrected standard rather than a real atmosphere is small.

Thus, a complete formula which gives the sky radiance, L_A , at the time of the ERTS overpass from L_{MEAS} made at another solar zenith angle and air mass is:

$$L_A = L_{MEAS}(\phi) \left[\frac{1 - \tau}{1 - \tau^{m_o}} \right] \frac{T_{ERTS}}{T_Z}, \quad (13)$$

in which ϕ , the scattering angle to the observer, equals the scattering angle to ERTS, and T_{ERTS} and T_Z are given by Equation 12 for the zenith angles at the time of the ERTS overpass and the time of the L_{MEAS} readings.

The validity of this equation is demonstrated in Figures 4 and 5. Figure 4 shows ground-based sky radiance measurements as a function of the scattering angle for a range of solar air masses. Each of the curves was obtained by pointing the RPMI at the sun and then sweeping it in azimuth and in elevation, taking sky radiance readings at 10° intervals. Alongside each curve, the solar air mass at the time of the observations is given. The curve defined by the open squares, which falls steeply, is for a range of solar air masses, and was produced by recording the zenith sky radiance over a period of several hours. Application of Equation 13 to these data in Figure 4, assuming $T_{ERTS} = 1$, gives the results shown in Figure 5. Except for about $\pm 5\%$ of scatter, all the points now follow the same line. By selecting L_A from the curve at the scattering angle which exists at the time of ERTS overpass and multiplying this value by T_{ERTS} , the desired value of L_A at the time of the ERTS overpass is determined.

For March, the path radiance was found to be equivalent to that produced by a target having a reflectance of 11% in Band 4, 5% in Band 5, 3% in Band 6, and 1% in Band 7. This radiance error, which varies as shown in Figure 5, is a function of scattering angle (sun angle), to some degree beam transmittance, and average surface reflectance.

GENERATION OF IMAGERY AND DATA CORRECTED FOR ATMOSPHERE

Different approaches for deriving target reflectance from ERTS data are being investigated. The approach that leads to the most accurate reflectance values is the application of Equation 4 and the full set of solar and atmospheric parameters (L_A , H_0 , τ , and H_{SKY}). The 27 March 1973 ERTS tape was processed in this manner to produce the color-coded imagery and gray-scaled computer printout of a portion of the ERTS scene shown in Figures 6 and 7. In this case, the color on the TV monitor and the symbol on the computer print-out is directly related to target reflectance. The scenes shown are those of Orchard Lake. The lake is approximately 2.4 km (1.5 miles) on a side and the scene is approximately 4.8 km (3 miles) on a side.

To obtain average reflectance and other statistical information (i. e., average counts, average radiance, standard deviations, etc.) on specific target areas, such as the deep water in Orchard Lake, etc., the gray-scale printout is used as a map to establish the coordinates of the target, using scan-line count and resolution element numbers. These coordinates, input to the computer, define data areas (edits) where the desired statistical computations are performed. Results of computations of average reflectance on deep water areas of six lakes established lake reflectance to be from 3 to 5.5% in Band 4, 0 to 2.3% in Band 5, 0 to 0.5% in Band 6, and 0 to 0.37% in Band 7. Spot reflectance measurements on the same lakes with the RPMI showed similar results.

EFFECTS OF ATMOSPHERE ON COMPUTER CLASSIFICATION TECHNIQUES

The ability of computer techniques to classify targets under various atmospheric conditions was studied. Training sets were defined for the eight land use categories shown in the tabulation of Figure 8 for 14 April 1973 ERTS tape acquired over Oakland County, Michigan. Data within the training areas were then used to generate a set of canonical coefficients (R. Dye 1970), one set for each land use category. In the target classification mode, these coefficients were used to form a linear combination of the ERTS measurement to produce a "canonical variable" whose amplitude is associated with the probability of an ERTS measurement being sought. The probability of each land use category being present within each ERTS element of the Oakland County scene is determined and a classified land use map is generated.

To determine how the atmosphere affected these classifications, the canonical coefficients generated from the April tape were first applied to classify the data from the known training areas also contained within this tape. This classification performance, recorded in the tabulation of Figure 8, then served as the basis from which to evaluate performance achieved when the same coefficients are used to process ERTS measurements on the identical targets observed under other atmospheric conditions. To accomplish this, the April observations from the training areas were modified to replace April atmospheric parameters with parameters derived from RPMI measurements for February, March, and May. These parameters are listed in Table 3. Also, the April atmospheric parameters were modified by incremental amounts to generate parametric curves of Figures 8A and 8B.

Figures 8A through 8E show the results of applying the processing coefficient derived for the 14 April atmosphere, denoted A_3 , to ERTS measurements acquired under other atmospheric conditions. Figure 8A shows how the classification performance degrades as the ratio of the April $H\tau$ to the new condition $H\tau$ increases when L_A is held constant. This is a parametric curve generated by modifying the April $H\tau$'s in each ERTS band by an equal amount. Figure 8B, also a parametric curve, shows the effect of increasing the differences between April path radiance values and new condition values, while holding $H\tau$ unchanged.

In Figure 8C and 8D, the February, March, April, and May atmospheres; denoted A_1 , A_2 , A_3 , and A_4 , respectively in Table 3; are used to evaluate the classification performance. In Figure 8C, as in Figure 8A, only $H\tau$ is permitted to vary but, in this case, the April $H\tau$'s are modified by the $H\tau$'s measured in February, March, and May. In Figure 8D, the effects of deviating the April path radiance by amounts equal to the difference in radiance between April and the other dates is shown.

Figure 8E shows classification accuracy achieved when April training (canonical coefficients) is used to process February, March, April, and May scenes in which the full atmospheres of those conditions prevail.

In Figure 8A through 8E, it is significant to note that the classification performance on some target categories (i. e., bare soil, tended grass, etc.) hold up even under the most severe atmospheres encountered, while the performance on other targets (trees, urban, untended grass, and deep water) degrades rapidly when atmospheric conditions change by the smallest amount from the reference condition (i. e., the condition in which the processing coefficients are generated).

Figure 9 shows the classified data of the April scene with February, March, April, and May atmospheres.

A set of canonical coefficients and target means derived from training areas within one ERTS scene, as shown, cannot be applied to process data from another ERTS scene with any degree of confidence unless the atmospheres within the two scenes are known to be essentially the same. N. J. Shah (1973) has established that the atmospheric parameters for both scenes can be used to modify the canonical coefficients and target means generated from one scene to process the data from the second scene.

Let H_1 , τ_1 , and L_{A1} be the atmospheric parameters applicable for an ERTS scene containing atmosphere I, for which training sets were previously selected and from which a canonical coefficients matrix C_1 and target means matrix X_1 were generated. Let H_2 , τ_2 , and L_{A2} be the atmospheric parameters for an ERTS scene with atmosphere II, in which additional processing is desired. The new canonical coefficient matrix, C_2 , for processing scene 2, is computed from the matrix C_1 by

$$C_2 = C_1 \left(\frac{H_2 \tau_2}{H_1 \tau_1} \right) \quad (14)$$

The new target means, denoted X_2 for scene 2, are related to means X_1 for scene 1 by

$$X_2 = X_1 \left(\frac{H_2 \tau_2}{H_1 \tau_1} \right) + L_{A2} - L_{A1} \left(\frac{H_2 \tau_2}{H_1 \tau_1} \right) \quad (15)$$

To illustrate the application of Equation 14 and 15, training and processing coefficients generated for the April scene together with the April and March atmosphere parameters were used to generate the new canonical coefficients and means needed to process the March tape. The results of this processing are shown in Figure 10A, an accurate classification of the original scene. Figure 10B shows the results of processing the same March tape, but using the April training and

coefficients without corrections for atmosphere. In this case, some lakes have been completely misclassified.

SUMMARY

Feasibility of the techniques for obtaining and using atmosphere parameters to transform spacecraft data into absolute target reflectance characteristics has been established. The RPMI's wide dynamic range (1×10^6) was found to be essential for obtaining the full set of measurements needed to derive atmospheric parameters.

The field measurements from January through June of 1973 determined the magnitude and range of variations in the beam transmittance, τ , and path radiance, L_A , within the ERTS bands. By generating coefficients needed to develop a land use map and, then, applying these coefficients to process ERTS scenes with new atmospheric conditions, the manner in which the atmospheric variations degrade classification performance was established. A simple technique for correcting these processing coefficients for atmospheric variations was shown.

REFERENCES

- S. Q. Duntley, J. I. Gordon, and J. L. Harris; Applied Optics; June 1973; "Measuring Earth-to-Space Contrast Transmittance from Ground Stations"; pgs 1317-1324.
- ERTS Data User Handbook; NASA Document 71SD4249; Revised Sept 1972; pg G-14.
- R. H. Rogers and K. Peacock; "Investigation of Techniques for Correcting ERTS Data for Solar and Atmospheric Effects"; NASA-CR-131258, E73-10458; April 1973.
- M. P. Thekaekara et al.; NASA Document SP-8005; Revised May 1971.
- S. L. Valley, Editor; Handbook of Geophysics and Space Environments; AFCRL; 1965; pgs 7-14 to 7-35.
- R. Rogers and K. Peacock; "Machine Processing of ERTS and Ground Truth Data"; Proceedings of Purdue LARS Conference on Machine Processing of Remotely Sensed Data; IEEE Catalog No. 73 CHO 834-26E; pgs 4a-14; Oct 1973.
- R. H. Dye and D. S. Hanson; "Spectral Signature Recognition"; Bendix Technical Journal, Vol 3, No. 2, Summer/Autumn 1970.
- N. J. Shah; "Using Reflectance in Producing Decision Imagery"; Bendix Memo 73-158-R and 0-635, 30 July 1973.

Table 1. Solar Irradiance Outside Atmosphere, H_0 (1AU)

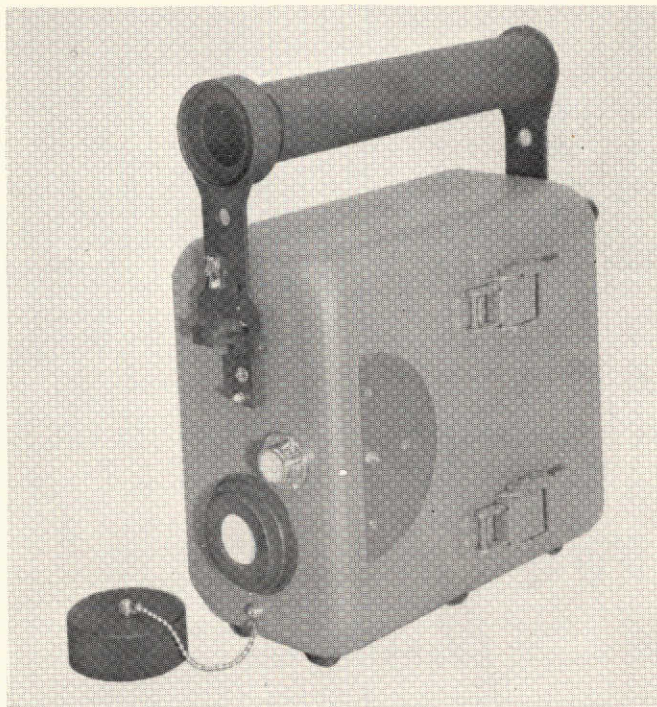
MSS Band	RPMI mW/cm ²	Thekaekara mW/cm ²
4	18.65	17.7
5	15.11	15.15
6	12.33	12.37
7	25.17	24.88

Table 2. Beam Transmittance, τ

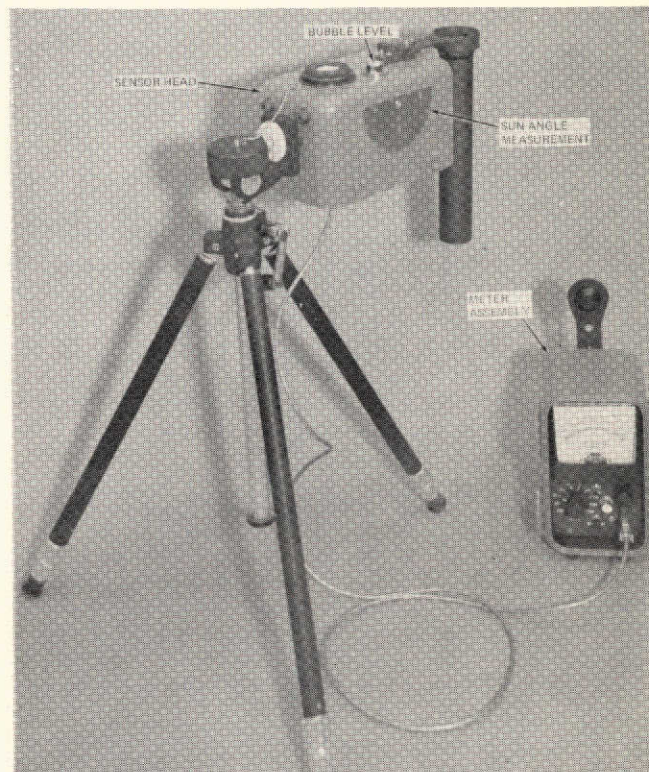
MSS Band	Average	Minimum	Maximum	Standard Deviation
4	0.799	0.697	0.856	0.051
5	0.852	0.770	0.901	0.048
6	0.885	0.812	0.940	0.051
7	0.899	0.843	0.975	0.052

Table 3. Atmospheric Parameters

Atmosphere	Date	Air Mass, M	Beam Transmittance, τ				Path Radiance L_A mw/cm ² -sr			
			4	5	6	7	4	5	6	7
A1	9 Feb 1973	2.5	0.856	0.901	0.940	0.975	0.27	0.146	0.093	0.1185
A2	27 Mar 1973	1.49	0.796	0.854	0.884	0.888	0.268	0.127	0.081	0.103
A3	14 Apr 1973	1.33	0.74	0.815	0.875	0.889	0.26	0.165	0.108	0.059
A4	21 May 1973	1.18	0.697	0.770	0.812	0.843	0.4	0.189	0.121	0.154



A. RPMI assembled.

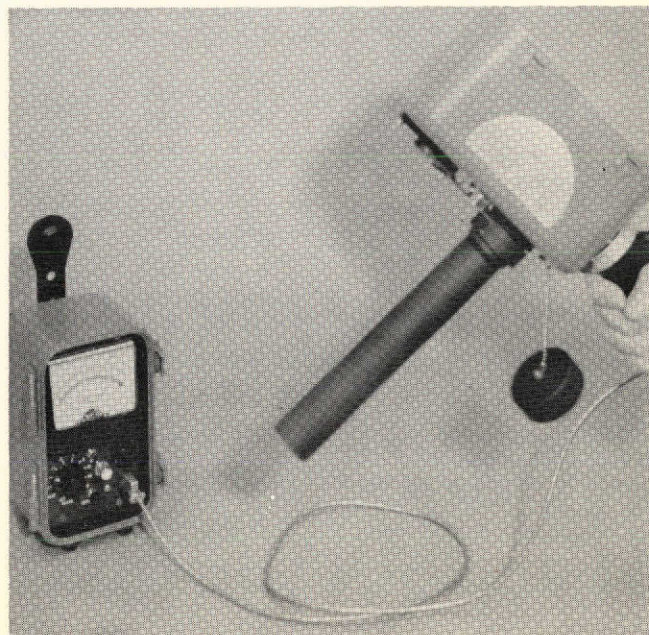


B. Global Irradiance (H) – 2π steradian field of view for measuring downwelling (incident) radiation ERTS MSS bands. Bubble level aids this measurement.

Sky Irradiance (H_{SKY}) – Block sun to measure global irradiance minus direct sun component, in every ERTS MSS band. Angle from zenith to sun is also measured in this mode by reading sun's shadow cast on sun dial.

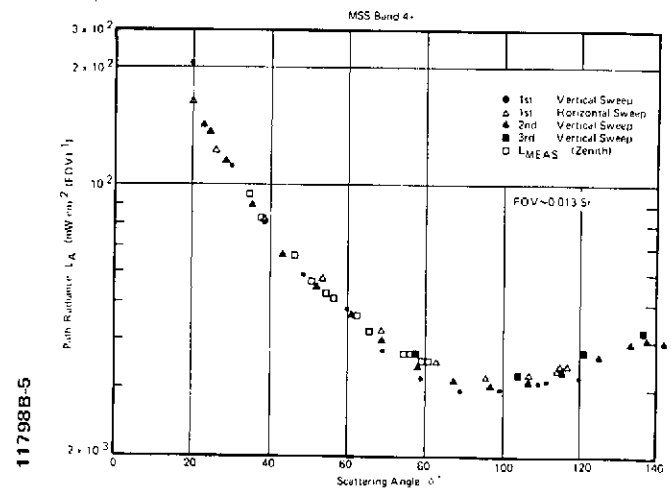
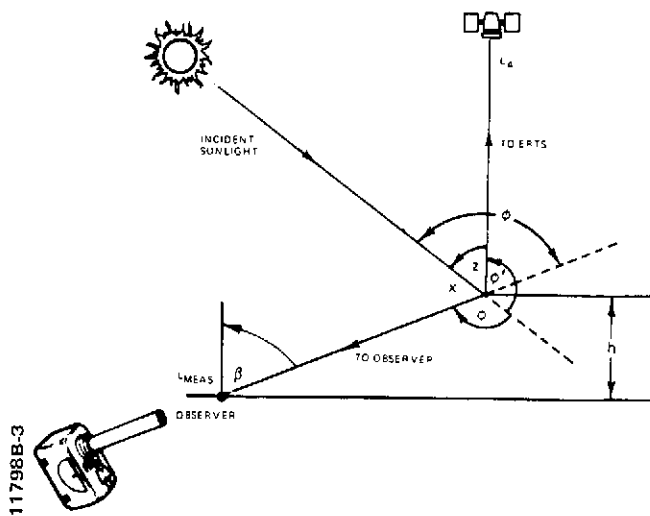
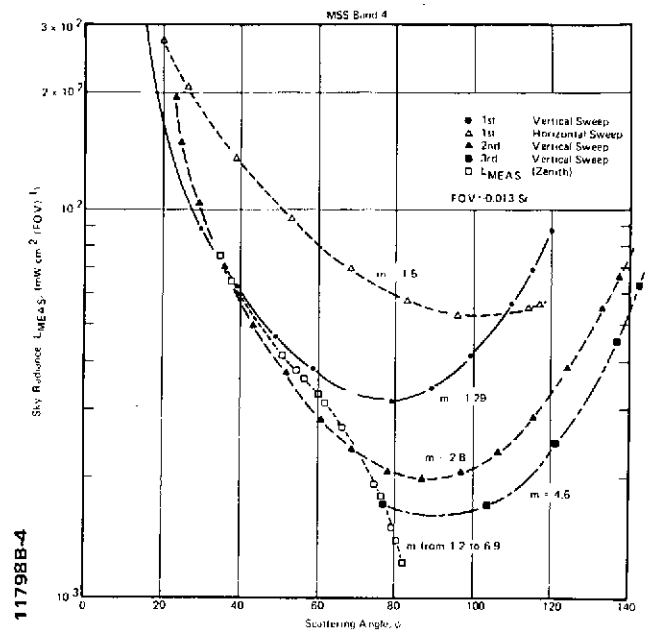
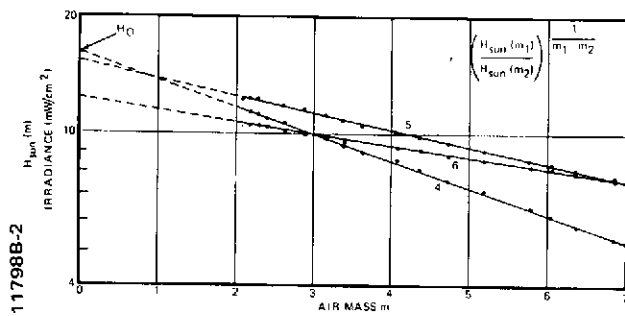


C. Radiance from Narrow Solid Angles of Sky (L_{MEAS}) – Handle serving as field stop permits direct measurements through a 7.0° circular field of view. This mode is also used to measure direct beam solar irradiance, H_{SUN} .



D. Reflected Radiation – Used with small calibration panels and cards to obtain direct measurement of truth site reflectance. Reflectance also immediately derived from ratio of reflected radiance and global irradiance.

Figure 1. Radiant Power Measuring Instrument



11798B-6



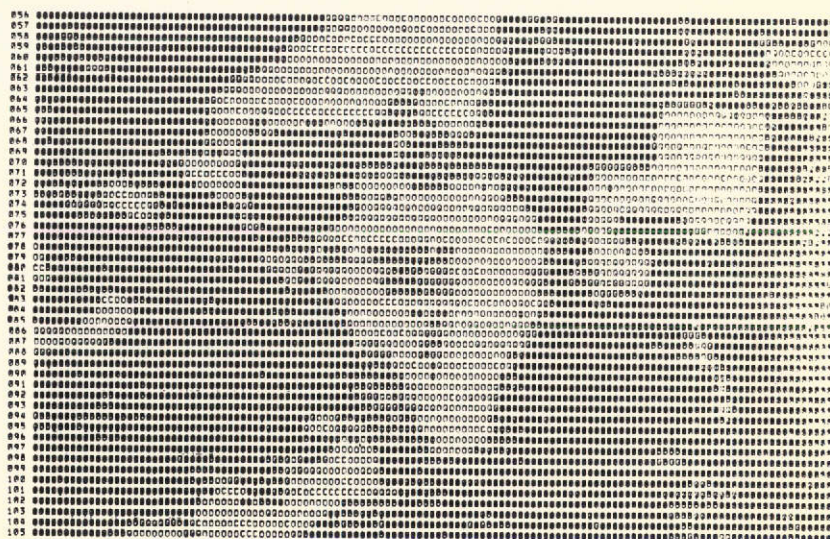
Aerial Photograph



ERTS Band 4 Display

Figure 6. Comparison of Aerial Photograph and Color-Coded TV Reflectance Display

Character	Reflectance Range
.	0.000 - 0.006
/	0.010 - 0.014
C	0.018 - 0.027
O	0.031 - 0.035
Q	0.039 - 0.047
@	0.051 - 0.055
9	0.059 - 0.067
B	0.071 - 0.075
0	0.079 - 0.087
8	0.091 - 0.095
6	0.099 - 0.100



Reflectance Gray Scale Printout
(Band 4)

Figure 7. Reflectance Gray-Scale Printout



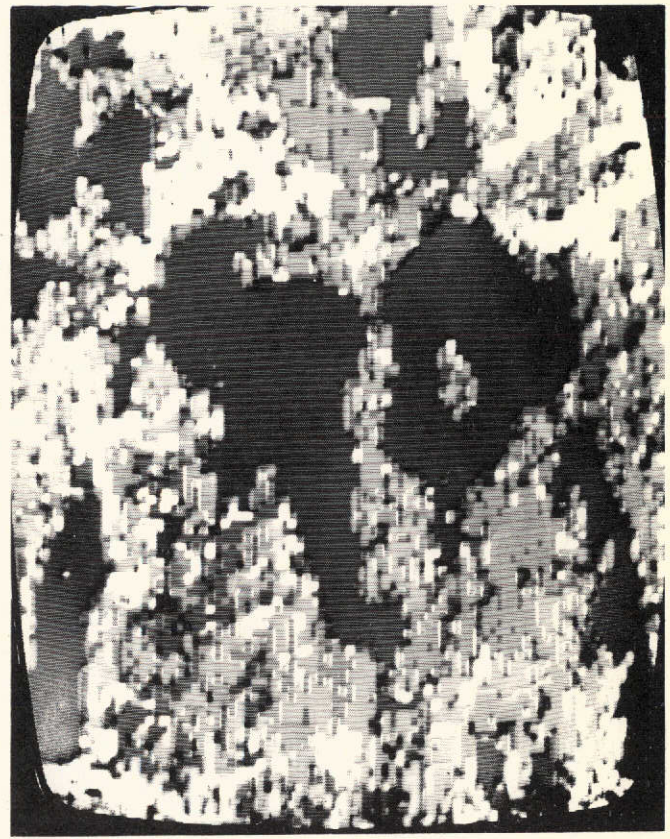
Reference Scene 14 April 1973; Atmosphere A3 τ_{avg} 0.83, L_{Aavg} 0.148 mw/cm² -sr



27 March 1973; Atmosphere A2 τ_{avg} 0.856, L_{Aavg} 0.145 mw/cm² -sr



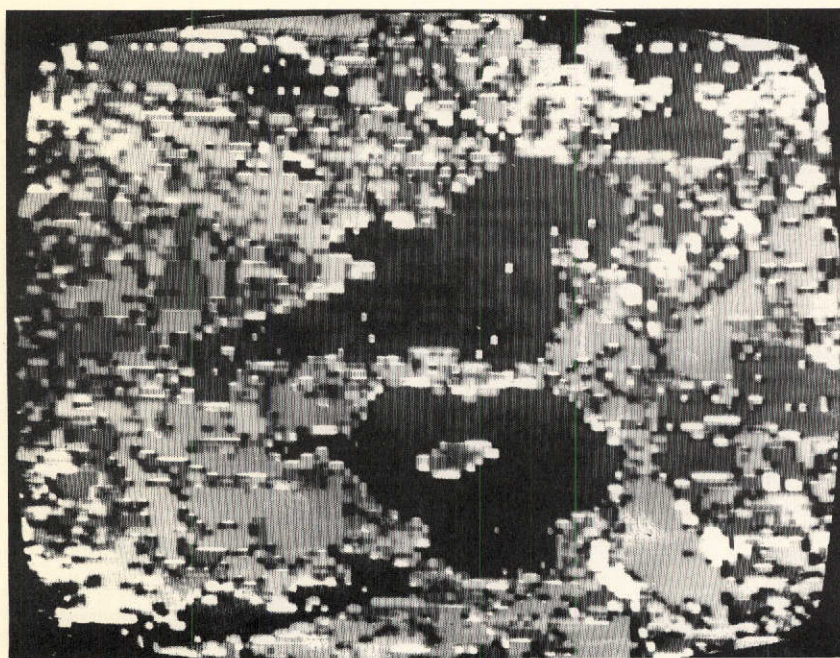
21 May 1973; Atmosphere A4 τ_{avg} 0.78, L_{Aavg} 0.216 mw/cm² -sr



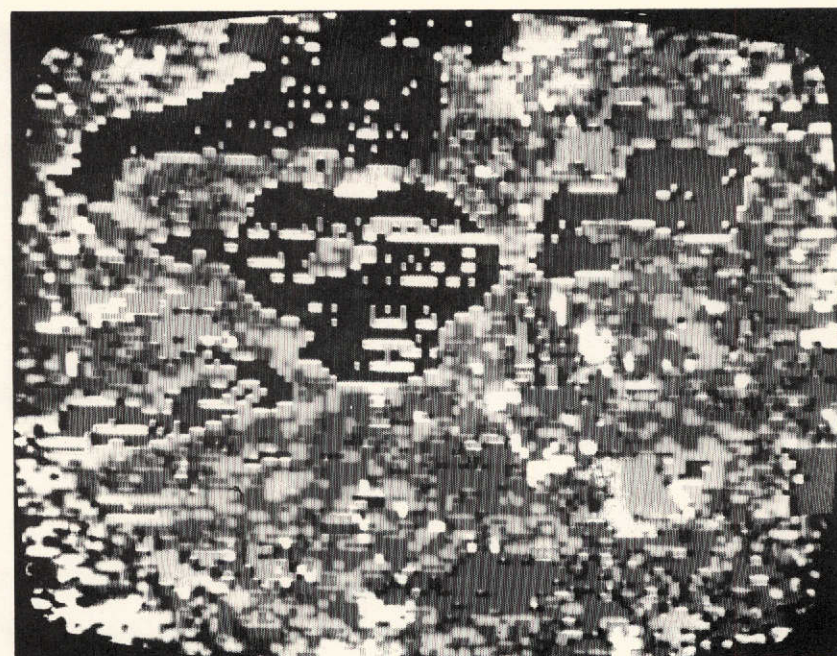
9 February 1973; Atmosphere A1 τ_{avg} 0.918, L_{Aavg} 0.157 mw/cm² -sr

Figure 9. Decision Processed Data Showing Atmospheric Effects on Decision Processing

11798B-10



Coefficients Corrected for Atmosphere



Coefficients Not Corrected for Atmosphere

Figure 10. March Scene Classified with April Processing Coefficients